JOURNAL OF MATERIALS SCIENCE 30 (1995) 2981-2988

Crystal growth of thin-plate β-alumina by liquid transport

M. USHIO
Department of Applied Chemistry, Faculty of Engineering, Gunma University, Tenjin-cho, Kiryu-shi, Japan

Single crystals of β-alumina ($Na_2O.11Al_2O_3$) were grown by liquid transport at 1030–1150 °C and for durations of 4–140 h, using an Na_3AlF_6 solvent and α- or β-alumina as the nutrient. The maximum size of β-alumina crystal grown using a small platinum crucible was 1.1 cm in length and 0.6 mm in thickness. On the other hand, a single crystal 1.8 m long and 0.7 mm thick was grown using a large crucible. These grown single crystals were hexagonal, thin platelike, and very transparent. Screw dislocation-like patterns were observed on the surfaces of grown β-alumina single crystals; each pattern showed a right-handed rotation. Small crystals on a matrix crystal grew spirally about the c-axis and formed a new, flat surface on the matrix crystal, evidently an intrusive twin. The angle between the two inclined crystals was ~ 2.9–2.8°. The twin face seemed to be w(14, 14, 3). The growth rates of β-alumina single crystals treated for less than 12 h using large and small crucibles were 3.3×10^{-1} and 4.0×10^{-1} mm h^{-1}, respectively. For treatment ranging from 12 to 40 h growth rates were 1.1×10^{-1} and 1.5×10^{-1} mm h^{-1} for the large and small crucible, respectively; rates for 40–100 h treatment were 0.3×10^{-1} mm h^{-1} for both crucibles. The grown β-alumina single crystals had fairly good crystallinity. The growth mechanism of the β-alumina single crystal can be estimated from transport through liquid film in the crucible, i.e. a creeping phenomenon.

1. Introduction

β-alumina has the chemical composition $Na_2O.11Al_2O_3$ and belongs to a hexagonal system with a space group $P6_3/mnnc(D^4_{6h})$. The crystal structure of β-alumina is shown in Fig. 1.

Recently, it has become clear that using β-alumina as a solid electrode component for a new type of battery would represent a notable, energy-saving technical development.

A previous paper [1] examined the growth of β-alumina by the Na_3AlF_6–NaF flux method, with special emphasis on the influence of sodium. A later paper [2] investigated the crystal growth process and growth conditions of β-alumina using the $Na_2B_4O_7$–Na_3AlF_6 flux method. In that study the weight loss of the flux varied widely for various runs: ≈ 10 wt % of flux evaporated at 100 h, ≈ 17 wt % at 150 h, and 43 wt % at 600 h. When β-alumina crystals were grown only 20 wt % $Na_2B_4O_7$ was added to the Na_3AlF_6 flux. The linear growth rates of the β-alumina single crystals grown by the Na_3AlF_6–20 wt % $Na_2B_4O_7$ flux method at 1040 °C and $\Delta t = 18$ °C were $\approx 1.0 \times 10^{-3}$ mm h^{-1} (a-face) and $\approx 0.3 \times 10^{-3}$ mm h^{-1} (c-face). The β-alumina single crystals grown were bounded by only c[001] and a[100] and were colourless and transparent.

The present paper investigates the growth of β-alumina by liquid transport using an Na_3AlF_6 solvent and α- or β-alumina as a nutrient. The growth conditions and rates for thin-plate β-alumina, surface observations for β-alumina, and β-alumina growth mechanisms, are examined.

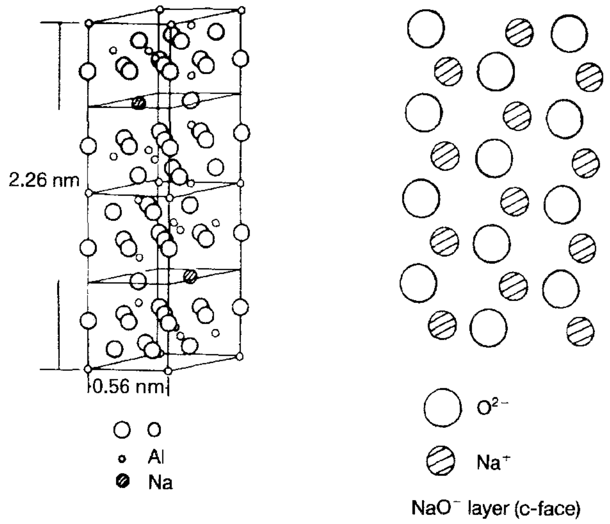

Figure 1 A crystal structure of β-alumina.

2. Materials and methods

The experimental apparatus consisted of two electric furnaces with Kanthal heaters: vertical and horizontal furnaces heated to 1150 and 600 °C, respectively. Two

0022-2461 © *1995 Chapman & Hall*

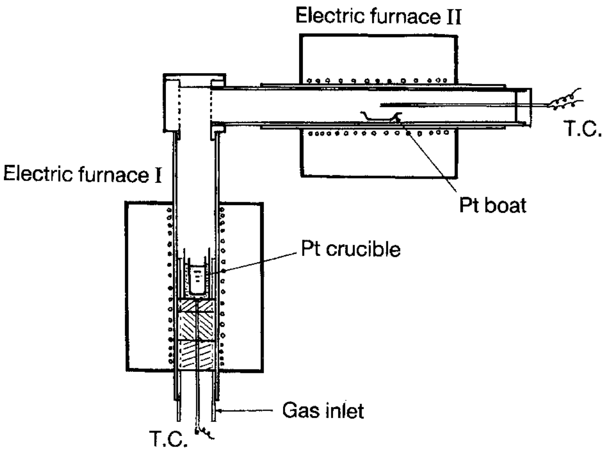

Figure 2 Experimental apparatus.

platinum crucibles were used, one 40 mm in diameter and 80 mm high and the other 60 mm in diameter and 150 mm high. Both a Pt–Pt13%Rh thermocouple and a chromel–alumel thermocouple were used for the temperature measurements given in Fig. 2.

A synthetic reagent, chryolite (Na_3AlF_6), was used as a flux. The nutrients were small single crystals of β-alumina selected from the block and a synthetic reagent β-alumina. A chromium oxide (Cr_2O_3) reagent was used as an additive to determine whether α- or β-alumina would grow.

The flux (120 g), a nutrient (40 g), and an additive (1.2 g) were placed in the small platinum crucible and set in the electric furnace(I) so that maximum heat would be at the bottom of the crucible. Three times more reagent was used for the large platinum crucible as for the small crucible. The temperature difference between the surface and bottom of the melt was ~ 2 °C. After the crucible had been heated to a predetermined temperature the furnace was regulated to achieve a temperature of 2 °C between the surface and the bottom of the melt, as argon gas flowed from the bottom of the furnace. The nutrient and additive were then dissolved into the flux melt, and after saturation the vapour of the melt flowed into both furnaces. The grown crystals were removed from the crucible, the boat, and the inner wall of the ceramic tube and washed in a hot, 6M-hydrochloride aqueous solution. Then the crystals were examined by X-ray diffraction (XRD), surface-finish microscopy, and scanning electron microscopy (SEM).

The Cr_2O_3 reagent was added to make the α-alumina and β-alumina distinguishable by colour; the α-alumina crystals were red and the β-alumina colourless. The two forms were also distinguishable by the shapes of their crystal faces.

3. Results

3.1. Experimental conditions and results

The experimental conditions and crystal growth results are shown in Table I. Very large single crystals of β-alumina grew mostly on the upper part and inner wall of the crucible, but very small crystals formed on the inner wall, part of the metal joint between the two furnaces, the boat, and the inner wall of the vertical ceramic tube. On the other hand a fine powder adhered to the metal joint and the inner wall of the horizontal ceramic tube.

The appearance of the melt after various stages of crystal growth is shown in Fig. 3. Most of the crystals grew on the upper part of the small crucible and covered this part. Fig. 3b shows the crystal appearance during growth, when the crystal growth rates were measured.

The large crystals from each run are shown in Fig. 4. For run A-10 (Fig. 4a) the maximum dimensions of the grown crystal were 1.1 × 0.6 mm. For run B-1 (Fig. 4b) crystals up to 1.8 cm long and 0.7 mm thick were grown. The grown crystals were hexagonal and thin, platelike and transparent.

3.2. Crystal growth in the direction of the a-axis

Size variations in the crystals that grew on the surface and near the centre of the crucible (Fig. 3b) were

TABLE I Growth of β-alumina

Run no.	Flux weight (g)	Nutrient weight (g)	Temperature (°C)	Time (h)	Gas (ml min^{-1})	Yield (g)	Alumina	Polycrystal	Single crystal	Maximum size of single crystal (mm)
Small platinum crucible										
A-1	120	40	1030	5	90	1.0	α	◎	○	0.1
A-2	120	40	1050	15	–	10.8	β		◎	6.0
A-3	120	40	1070	30	–	4.2	β	◎		0.1
A-4	120	40	1080	10	60	0.1	α	◎		0.1
A-5	120	40	1100	37	–	1.6	β	◎	○	5.0
A-6	120	40	1100	50	–	5.0	β	◎	○	1.2
A-7	120	40	1120	75	–	9.0	β	◎	○	0.4
A-8	120	40	1140	50	90	9.5	β	◎	○	0.3
A-9	120	40	1150	23	–	1.2	β		◎	6.0
A-10	120	40	1150	90	–	8.2	β		◎	11.2
Large platinum crucible										
B-1	360	120	1100	140	–	32.6	β		◎	18.0
B-2	360	120	1100	140	–	40.1	β		◎	16.5

◎, large quantity; ○, small quantity

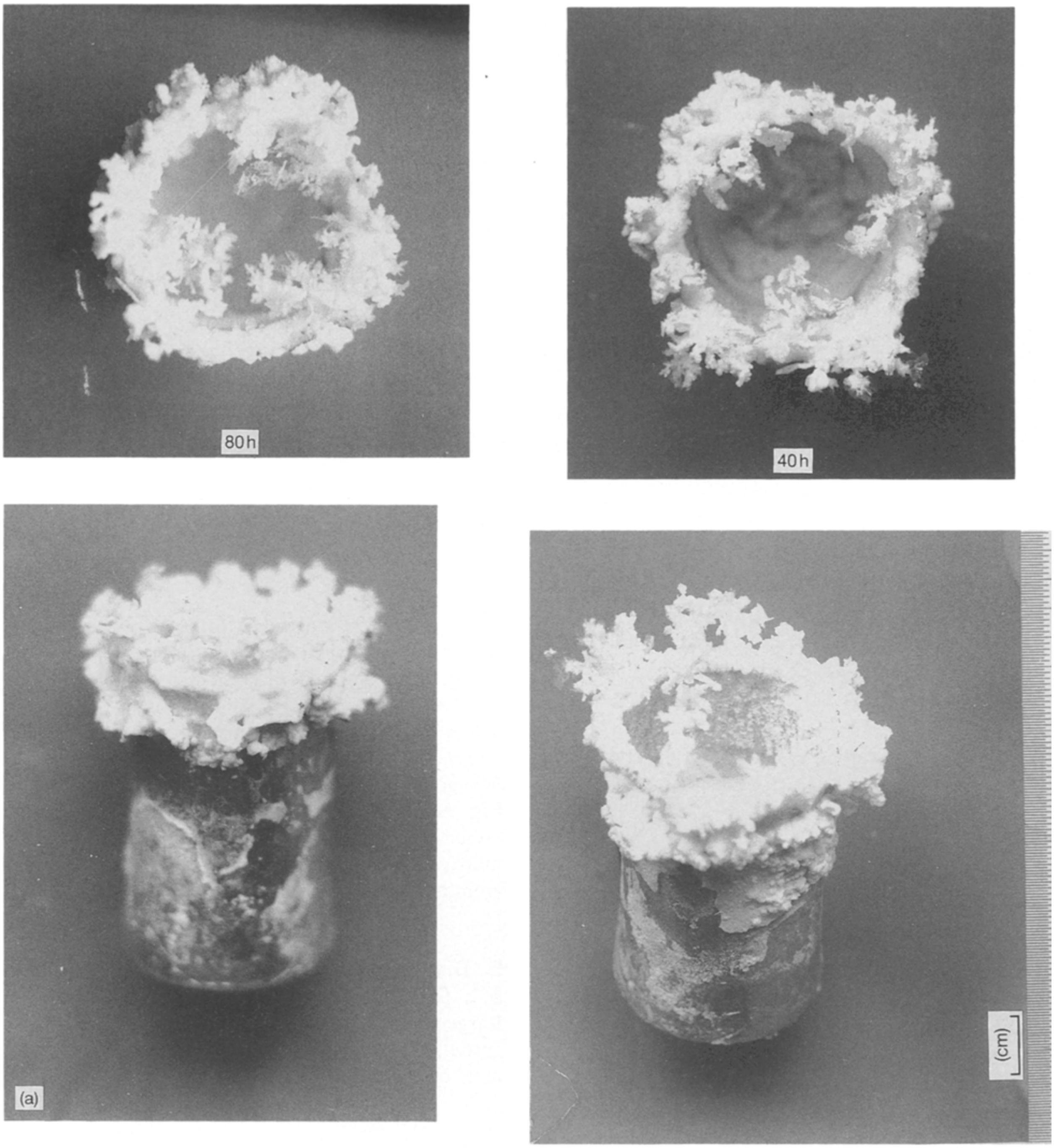

Figure 3 (a) Appearance after various stages of growth for run (A-10), (b) Enlarged photo for run (A-10).

measured against growth time; these results are shown in Fig. 5. No crystals longer than 9 mm were attained in the small crucible, and none longer than 1.1 cm formed in the large crucible.

Crystal size increased with growth time, but it can be assumed that no crystals grew after 100 h of treatment time.

3.3. X-ray powder diffraction pattern and Laue photograph

The transparent grown crystals were cut into small pieces and examined by X-ray powder diffraction (XRPD); an XRPD pattern for run A-10 is shown in Fig. 6. The 2 θ values and the intensities of all peaks were in agreement with those of the reference samples [3]. It can therefore be assumed that the grown crystals were β-alumina. A Laue photograph of the crystal grown for run A-10 is shown in Fig. 7. The X-ray was irradiated normal to the c-face. A sixfold symmetry is observed in the strongest spots.

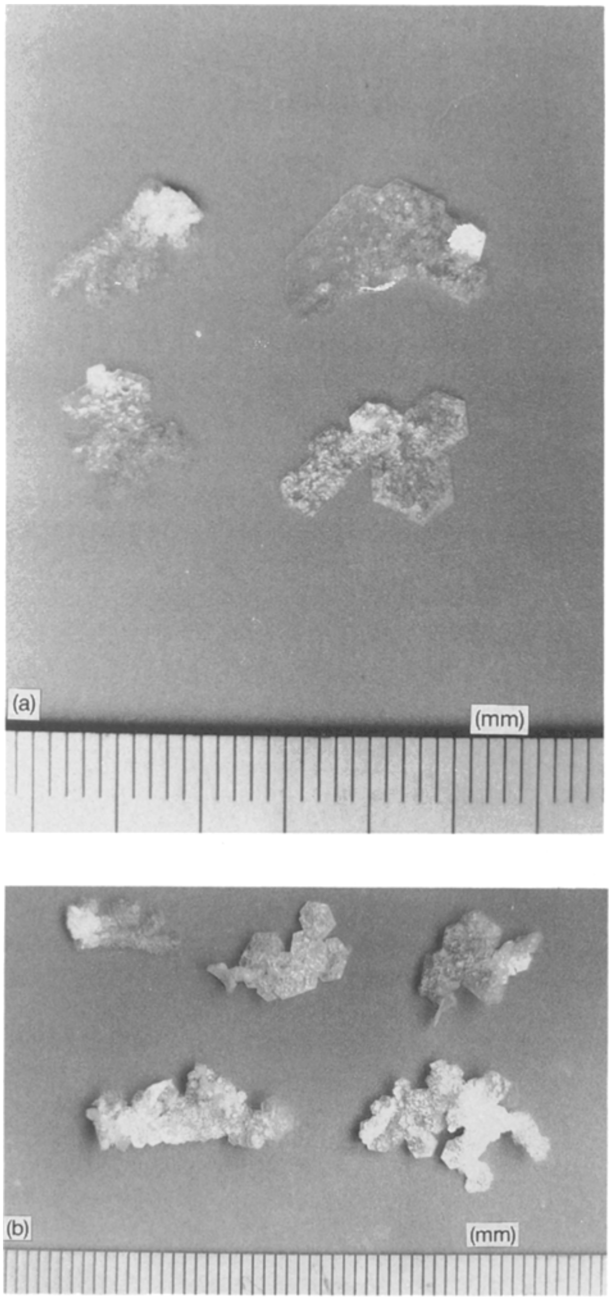

Figure 4 Grown single crystals of β-alumina: (a) run (A-10); (b) run (B-1).

4. Observations by surface-finish microscopy and SEM

The results of observation by surface-finish microscopy are shown in Fig. 8. Screw dislocation-like patterns were observed here and there on the surfaces of the grown crystals. The grown crystal in Fig. 8a, however, was verified twin crystals, whereas the crystals in Fig. 8b and c could have been grown by screw dislocations.

The SEM photographs of the grown crystals are shown in Fig. 9. In Fig. 9a the crystals grow spirally about the c-axis. The enlarged photograph (Fig. 9b) shows that the grown crystals were ~ 12 μm thick and that each c-face was inclined from the others. The angles between the sides and the c-faces of the grown crystals were 90° and the angles between the two sides were 120°. Small crystals on the matrix crystal grew spirally about the c-axis and formed a new, flat surface on the matrix crystal, as shown in Fig. 9c.

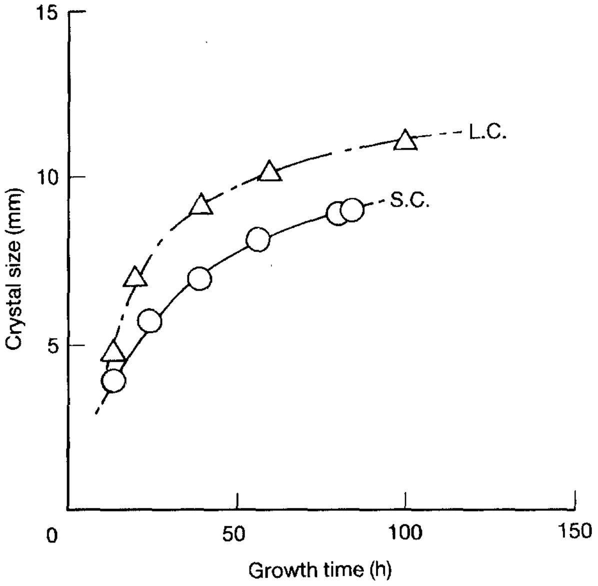

Figure 5 Crystal-size variation of β-alumina single crystal on the surface of large platinum crucible (L.C) and small platinum crucible (S.C.).

Fig. 9d shows small hexagonal crystals growing on the c-face of the matrix crystal (two enlarged photos). These small crystals were formed spirally about the c-axis, and each c-axis was curved to the others. The hexagonal crystal that grew on the matrix crystal in Fig. 9e consisted of several small crystals. The enlarged photo (bottom) shows that the surface of the matrix crystal is flat except for the very small β-alumina crystals.

5. Discussion

5.1. Crystal growth of β-alumina

Large single crystals of β-alumina thus grew almost entirely on the upper part and inner wall of the platinum crucible. The maximum length of the crystals grown was 1.1 cm in the small crucible but in the large crucible 1.8 cm long crystals were grown.

If the amount of vapour evaporation from the surface of the melt per unit of cross-section is constant, it can be assumed that larger crystals will grow in the large crucible, with a cross-section 2.3 times larger than that of the small one.

5.2. Crystal growth rate in the direction of the a-axis

As shown in Fig. 5, crystals up to 9 mm long could be obtained in a small crucible and crystals 1.1 cm long in a large one. Below 12 h the growth rates of the crystals in the large and small crucibles were 3.3×10^{-1} and 4.0×10^{-1} mm h^{-1}, respectively. For times ranging from 12 to 40 h the growth rates were 1.1×10^{-1} and 1.5×10^{-1} mm h^{-1}, respectively. Growth rates for times ranging between 40 and 100 h were 0.3×10^{-1} mm h^{-1} for both crucibles. These growth rates are two orders of magnitude larger than those obtained by the flux method [2].

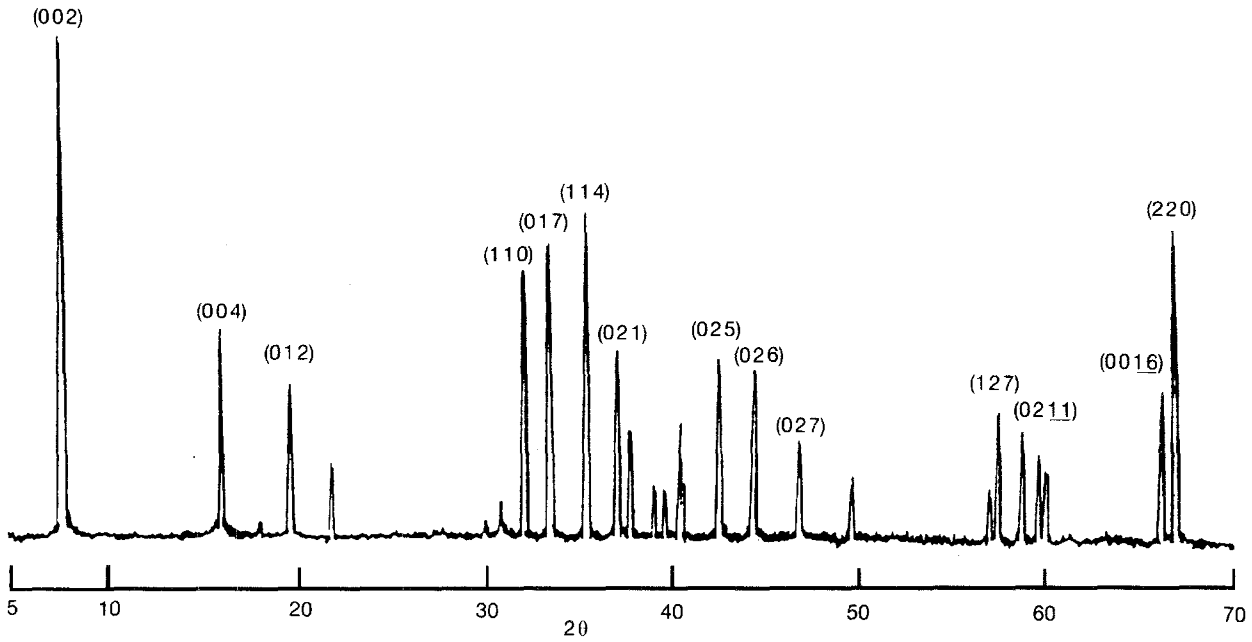

Figure 6 X-ray powder diffraction pattern for run (A-10).

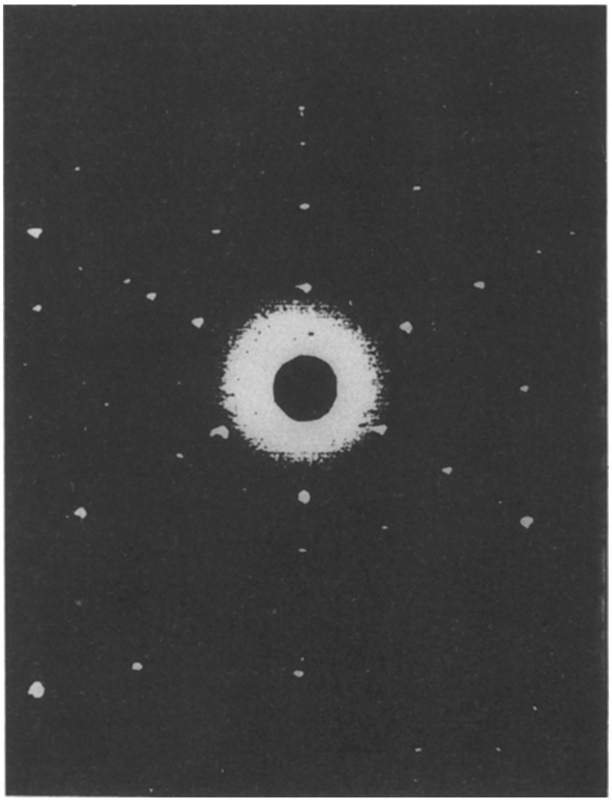

Figure 7 Lave photograph normal to c-face for run (A-10).

5.3. XRPD pattern and Laue photograph

All peaks ((0 0 2), (0 0 4), (0 1 2), (1 1 0), (0 1 7), (1 1 4), (0 2 1), (0 2 5), (0 2 6), (1 2 7), (2 2 0)) belonged to the diffraction lines of β-alumina. No unknown peaks were recognized.

From the Laue photograph spots of (0 1 2), (0 2 1), (1 1 0), were strong and sixfold symmetry was observed. It can be assumed that the grown crystals exhibited good crystallinity.

5.4. Surface observation of grown β-alumina crystals

Fig. 8a shows both large and small hexagonal crystals growing spirally about a particular c-axis, just like a card put obliquely between another basal card. Apparently this formation was an intrusive twin. The angle between the two inclined crystals was 4.8°.

Screw dislocation-like patterns are observed in Fig. 8b and c, and each pattern shows a right-handed rotation.

The SEM photographs of the grown crystals show the spiral growth rounded about a c-axis in Fig. 9. Fig. 9c, especially, shows small crystals on the matrix β-alumina crystal growing spirally about the c-axis. The angle between the two inclined crystals is 2.9°–3.6°. Subconchoidal to uneven fracture apparently is observed, and the twin face seems to be w(14, 14, 3).

6. Growth mechanism of β-alumina single crystals

It is very difficult to determine the growth mechanism of β-alumina single crystals. Firstly, the dissociation mechanism of the Na_3AlF_6–Al_2O_3 system in a state of melt was assumed because a small quantity of β-alumina single crystal was grown in the electric furnace (II) and on a corner between the electric furnace (I) and (II).

For the Na_3AlF_6–Al_2O_3 system Boner [4] reported dissociation according to the equation

$$5Na_3AlF_6 + 2Al_2O_3 \rightarrow 3Na_3AlF_6 + 6NaAlOF_2 \qquad (1)$$

On the other hand, Frank and Foster [5] proposed the following equilibria

$$\begin{array}{ccc} 2Na_3AlF_6 + 2Al_2O_3 & \rightarrow & 6NaAlOF_2 \\ \downarrow\uparrow & & \downarrow\uparrow \\ 4NaF + NaAlF_4 & & 3NaAlO_2 + 3NaAlF_6 \end{array} \qquad (2)$$

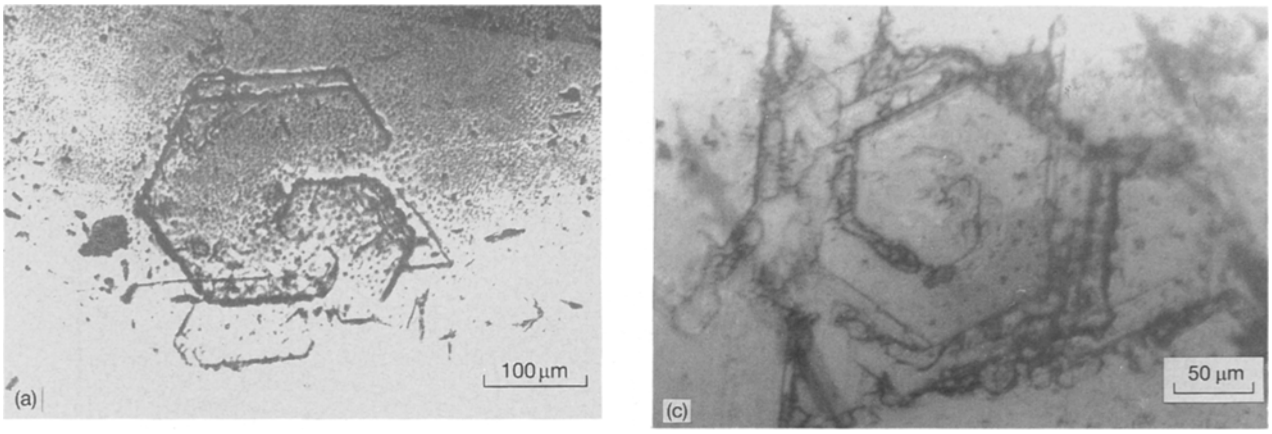

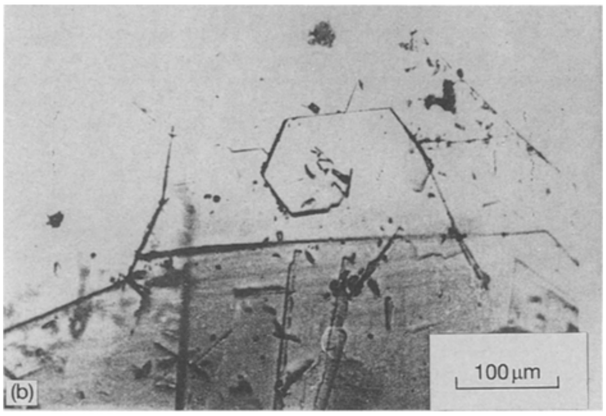

Figure 8 Micrographs of β-alumina single crystals for run (A-10).

or

$$\begin{array}{ccc} 5Na_3AlF_6 + 2Al_2O_3 \rightarrow & 3Na_3AlO_2F_2 & + 6NaAlF_6 \\ \downarrow\uparrow & & \downarrow\uparrow \\ 10NaF + 5NaAlF_4 & & \#NaAlO_2 + 6NaF \end{array} \quad (3)$$

The vapour pressures [6] of $NaAlF_4$, Na_3AlF_4, NaF, and AlF_3 at 1000 °C are 78 mmHg (10.4 kPa), 1.6 mmHg (0.21 kPa), 0.2 mmHg (0.027 kPa), and 11 mmHg (1.47 kPa), respectively. On the other hand the vapour pressure of NaF is 0.499 mmHg (0.067 kPa) at 1300 K [7]. Because the vapour pressure of NaF is very low (lower than that of $NaAlF_4$), it seems that NaF evaporation is difficult to achieve.

The following equations (vapour phases) apparently occur

$$22NaAlO_2 + 10NaAlF_4 \rightarrow Na_2O.11Al_2O_3 + 20NaF + 10NaAlOF_2 \quad (4)$$

or

$$22NaAlO_2 + 5NaAlF_4 \rightarrow Na_2O.11Al_2O_3 + 10NaF + 10Na_3AlO_2F_2 \quad (5)$$

As the compounds of $NaAlOF_2$ and $Na_3AlO_2F_2$ dissociated to $NaAlO_2 + NaAlF_4$ and $NaAlO_2$, respectively, the above two equations coordinate to the following

$$17NaAlO_2 + 5NaAlF_4 \rightarrow Na_2O.11Al_2O_3 + 20NaF \quad (6)$$

In other words, β-alumina can grow.

7. Conclusions

Large amounts of big β-alumina can grow by liquid transport at 1030–1150 °C and for durations of 4–140 h, using an Na_3AlF_6 solvent and α- or β-alumina as the nutrient. With a small crucible maximum dimensions of grown β-alumina single crystals were 1.1 cm length and 0.6 mm thickness. On the other hand, single crystals up to 1.8 cm long and 0.7 mm thick were grown using a large platinum crucible. These single crystals were hexagonal, thin, plate-like and transparent. Screw dislocation-like patterns were observed on the surface of the grown β-alumina crystals. Small crystals on a matrix crystal grew spirally about the c-axis and formed a new, flat surface on the matrix crystal.

The growth rates of β-alumina single crystals treated for less than 12 h in both large and small crucibles were 3.3×10^{-1} and 4.0×10^{-1} mm h^{-1}, respectively. For times ranging from 12 to 40 h, in both crucibles, the growth rates were 1.1×10^{-1} and 1.5×10^{-1} mm h^{-1}, respectively. Growth rates for times ranging from 40 to 100 h were 0.3×10^{-1} mm h^{-1} for both crucibles.

A Laue photograph showed fairly good crystallinity for the grown β-alumina single crystals. Apparently, the formation was an intrusive twin. The angle between the two inclined crystals was 2.9°–4.8°; the twin face seemed to be w(14, 14, 3).

The growth mechanism of the β-alumina single crystals grown by the vapour phase method can be estimated from the vapour pressure of each compound by the equations

$$22NaAlO_2 + 10NaAlF_4 \rightarrow Na_2O.11Al_2O_3 + 20NaF + 10NaAlOF_2$$

Figure 9 Scanning electron micrographs of β-alumina single crystals for run (A-10).

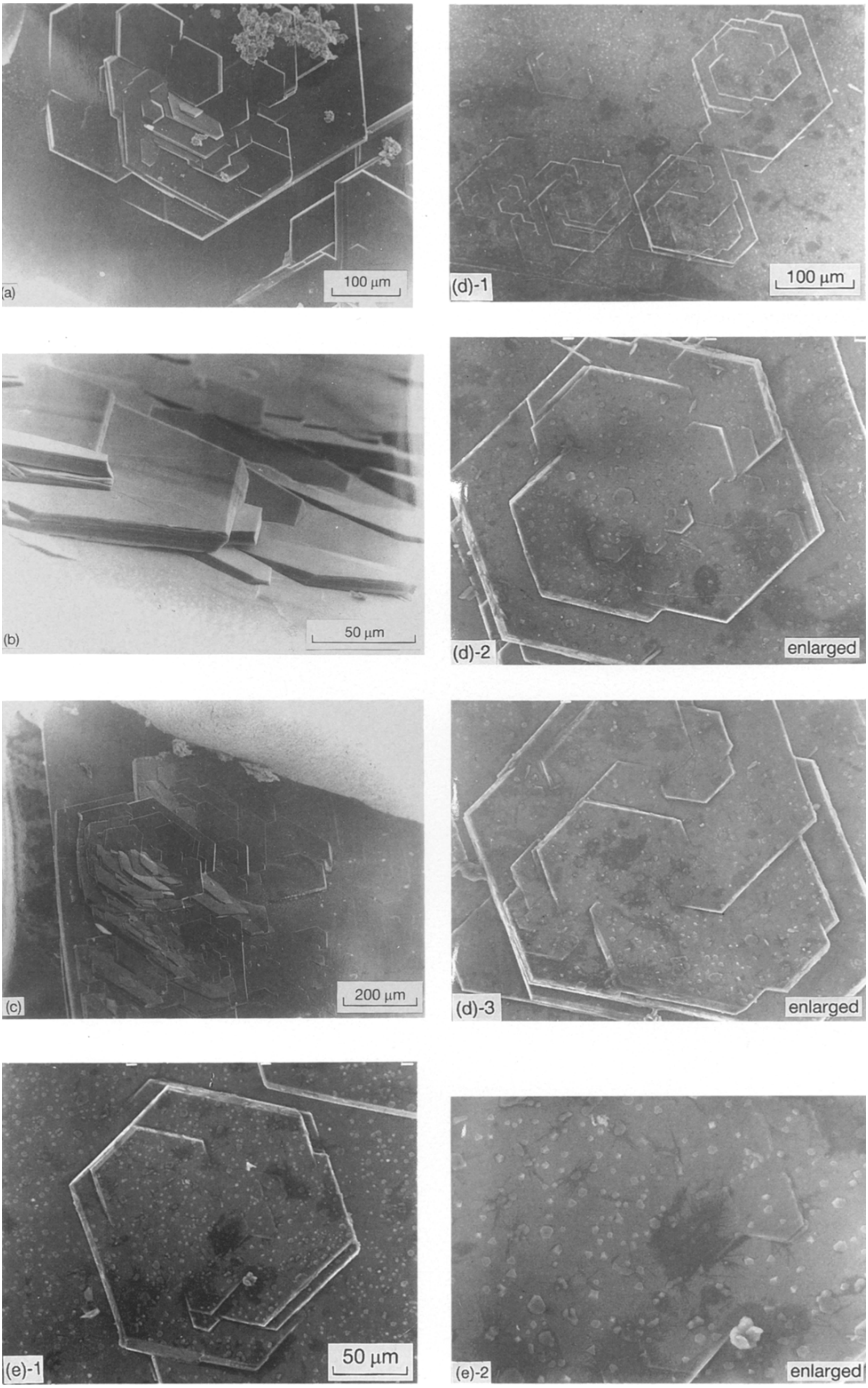
(a)
100 μm
(d)-1
100 μm
(b)
50 μm
(d)-2
enlarged
(c)
200 μm
(d)-3
enlarged
(e)-1
50 μm
(e)-2
enlarged

or

$$22NaAlO_2 + 5NaAlF_4 \rightarrow Na_2O.11Al_2O_3 + 10NaF + 10Na_3AlO_2F_2$$

These two equations can be coordinated by the equation

$$17NaAlO_2 + 5NaAlF_4 \rightarrow Na_2O.11Al_2O_3 + 20NaF$$

For large grown β-alumina single crystal, however, the growth mechanism can be estimated by a liquid transport method, i.e. a creeping phenomenon.

Acknowledgments

The author is grateful to Mr Kohji Mabuchi for his assistance in the synthesis of the single crystals.

References

1. Y. SUMIYOSHI, M. USHIO and M. NISHIMURA, *J. Chem. Soc. Jpn* (1987) 1001.
2. Y. SUMIYOSHI and M. USHIO, *J. Amer. Ceram. Soc.* **73** (1990) 3015.
3. ASTM card 25–774.
4. J. B. BONER, *Helv. Chim. Acta.* **33** (1950) 1137.
5. W. B. FRAK and L. H. FOSTER, *J. Phys. Chem.* **61** (1957) 1531.
6. M. H. VETYUKOV, M. L. BLYUSHTEIN and V. P. PODDYMOV, *Izvest. Vysshikh Ucheb. Zavedenix, Jsvetnaya Met* **2** (1959) 1137.
7. I. BARIN and O. KNACHE, "Thermochemical Properties of Inorganic Substances" (Springer-Verlag, Berlin–Heidelberg–New York, 1973).

Received 5 April 1993
and accepted 9 June 1994